Z boson radiative decays to a *P*-wave quarkonium at NNLO and LL accuracy

Wen-Long Sang,[1,*] De-Shan Yang,[2,†] and Yu-Dong Zhang[1,‡]

[1]*School of Physical Science and Technology, Southwest University, Chongqing 400700, China*
[2]*School of Physical Sciences, University of Chinese Academy of Sciences, Beijing 100049, China*

(Received 26 August 2022; accepted 1 November 2022; published 22 November 2022)

In this work, we study the radiative decay of a Z boson to a P-wave quarkonium H in association with a photon, where H can be χ_{QJ}, h_Q with $Q = c, b$ and $J = 0, 1, 2$. The helicity amplitudes and the unpolarized decay widths are evaluated up to QCD next-to-next-to-leading order (NNLO) within the framework of nonrelativistic QCD (NRQCD). For the first time, we check the NRQCD factorization for h_Q exclusive production at two-loop order. The leading logarithms (LL) of m_Z^2/m_Q^2 in the leading-twist short-distance coefficients, which may potentially ruin the perturbative convergence, are resummed to all orders of α_s by employing the light-cone factorization. We find the radiative corrections are considerable for χ_{Q2} and h_Q productions, while they are moderate or even minor for other channels. We also notice that the LL resummation can change the leading-order predictions for decay widths by more than 25% for $\chi_{c0,2}$ and h_c productions, and by around 50% for χ_{c1} production. However, effects of the LL resummation on the next-to-leading-order and NNLO predictions are notably mitigated. Some phenomenological explorations are also performed.

DOI: 10.1103/PhysRevD.106.094023

I. INTRODUCTION

The radiative decay of a Z boson to a quarkonium serves as an ideal platform to study the interplay of the perturbative and nonperturbative nature of QCD. To date, experimentalists have made many endeavors to search for such processes [1–3], yet failed to find any signals. In recent years, several high-luminosity lepton colliders are proposed, such as `ILC` [4], `FCC-ee` [5], and `CEPC` [6], which are planned to run at Z mass pole for a period of time. Undoubtedly, tremendous Z bosons will be accumulated. Thus it will provide more opportunities to probe these rare decay processes.

The exclusive processes $Z \to \text{quarkonium} + \gamma$ have been extensively studied on the theoretical side. The computation on these processes can date back to the earlier 1980s by the authors in Ref. [7]. In Ref. [8], these processes have also been studied at the lowest order in α_s and v^2 in both the nonrelativisitic QCD (NRQCD) [9] and the light-cone (LC) factorization formalisms [10,11], where v represents the typical velocity of the heavy quark in the quarkonium rest frame. In Ref. [12], the analytic expressions of the amplitudes for $Z \to \text{quarkonium} + \gamma$ were obtained in the leading-power LC approximation at next-to-leading order (NLO) in α_s. In Ref. [13], calculations of the rates for $Z \to V + \gamma$, where V signifies a vector quarkonium J/ψ or Υ, were presented. The calculations were accurate up to the leading-power LC approximation at the NLO in α_s and v. Shortly afterwards, the decay rates for $Z \to V + \gamma$ were restudied in Ref. [14], where the resummation of the leading logarithms (LL) of m_Z^2/m_Q^2, with m_Z and m_Q being the masses of the Z boson and heavy quark Q, respectively, were carried out. In Ref. [15]. the authors have further considered the resummation of logarithms of m_Z^2/m_Q^2 for the $\mathcal{O}(\alpha_s)$ corrections as well as the $\mathcal{O}(v^2)$ corrections. Very recently, the decay rates for $Z \to \Upsilon(nS) + \gamma$ have been calculated up to NLO in α_s based on the NRQCD, which are proposed to determine the $Zb\bar{b}$ coupling [16]. As relevant studies, the cross sections of $e^+e^- \to \text{charmonium} + \gamma$ at Z factories have been computed at LO and NLO in α_s in Ref. [17] and in Ref. [18], respectively, and the cross sections of $e^+e^- \to \text{bottomonium} + \gamma$ at Z factories have been studied in Ref. [19].

In this work, we study the processes of Z boson radiative decays to a P-wave quarkonium, i.e., $Z \to H + \gamma$, where H can be χ_{QJ}, h_Q with $Q = c, b$ and $J = 0, 1, 2$. Based on the NRQCD factorization and helicity formulas, we compute

*wlsang@swu.edu.cn
†yangds@ucas.ac.cn
‡zhangyudong@email.swu.edu.cn

the various helicity amplitudes at next-to-next-to-leading order (NNLO) in α_s and leading order (LO) in v. Since the two typical energy scales m_Q and m_Z involved in these processes are widely separated, the NRQCD short-distance coefficients (SDCs) receive contributions from large logarithms of m_Z^2/m_Q^2, which may potentially ruin the perturbative convergence in α_s. Fortunately, it was pointed out [20] that the NRQCD SDCs can be refactorized in the framework of LC formalism, in which the large logarithms can be resummed by employing the celebrated Efremov-Radyushkin-Brodsky-Lepage (ERBL) equation [10,21]. We will carry out the LL resummation for the leading-twist helicity amplitudes. Thus our computation for $Z \to H + \gamma$ will be at NNLO in α_s at fixed-order accuracy, meanwhile at all orders in α_s at LL accuracy.

The rest of the paper is organized as follows. In Sec. II, we employ the helicity amplitude formalism to analyze the $Z \to H + \gamma$ processes and build the polarized and unpolarized decay rates out of various helicity amplitudes. In Sec. III, we factorize the helicity amplitudes by employing the NRQCD factorization formalism and parametrize the corresponding SDCs through NNLO in α_s. The key technical ingredients of extracting the SDCs affiliated with each helicity amplitude through α_s^2 are sketched, and values of the SDCs at various perturbative levels are presented. The corresponding details about constructions of all the helicity projectors are presented in Appendix. We devote Sec. IV to the LC factorization for the leading-twist helicity SDCs. The resummation of the LL is formulated and explicitly carried out. In Sec. V, a detailed phenomenological analysis is performed. Finally, we summarize in Sec. VI.

II. THE GENERAL FORMULA

It is convenient to employ the helicity amplitude formalism to analyze the hard exclusive production process. The differential decay width of the Z boson with polarization (along the z axis) S_z into a quarkonium H and a photon, the helicities of which are λ_1 and λ_2, respectively, can be expressed as [22,23]

$$\frac{\mathrm{d}\Gamma}{\mathrm{d}\cos\theta}(Z(S_z) \to H(\lambda_1) + \gamma(\lambda_2)) = \frac{|\mathbf{P}|}{16\pi m_Z^2} |d^1_{S_z,\lambda_1-\lambda_2}(\theta)|^2 |A^H_{\lambda_1,\lambda_2}|^2, \quad (1)$$

where $\mathbf{P}$ denotes the spatial components of the H momentum, $\mathcal{A}^H_{\lambda_1,\lambda_2}$ represents the amplitude corresponding to the helicity configuration (λ_1, λ_2), and $d^1_{S_z,\lambda_1-\lambda_2}(\theta)$ is the Wigner function. Here, θ is the angle between the direction of $\mathbf{P}$ and the z axis. Note that the constraint, $\lambda_1 - \lambda_2 \le 1$, is guaranteed by the angular momentum conservation. The magnitude of the spatial momentum $|\mathbf{P}|$ is readily determined via

$$|\mathbf{P}| = \frac{\lambda^{1/2}(m_Z^2, m_H^2, 0)}{2m_Z} = \frac{m_Z^2 - m_H^2}{2m_Z}, \quad (2)$$

where m_H denotes the mass of the quarkonium H and the Källen function is defined via $\lambda(x, y, z) = x^2 + y^2 + z^2 - 2xy - 2xz - 2yz$.

Integrating over the polar angle θ and averaging over the polarization of Z, we finally obtain the integrated decay width of $Z \to H + \gamma$ for the helicity configuration (λ_1,λ_2) as

$$\Gamma(Z \to H(\lambda_1) + \gamma(\lambda_2)) = \frac{|\mathbf{P}|}{24\pi m_Z^2} |A^H_{\lambda_1,\lambda_2}|^2. \quad (3)$$

Thanks to the parity invariance [22], we have the following relations:

$$A^{\chi_{QJ}}_{\lambda_1,\lambda_2} = (-1)^J A^{\chi_{QJ}}_{-\lambda_1,-\lambda_2}, \qquad A^{h_Q}_{\lambda_1,\lambda_2} = A^{h_Q}_{-\lambda_1,-\lambda_2}. \quad (4)$$

Thus the number of independent helicity amplitudes for χ_{Q0}, χ_{Q1}, χ_{Q2}, and h_Q production can be reduced to one, two, three, and two, respectively.

In the limit of $m_Z \gg m_Q$, the helicity amplitude $A^H_{\lambda_1,\lambda_2}$ satisfies the asymptotic behavior

$$A^H_{\lambda_1,\lambda_2} \propto r^{1+|\lambda_1|}, \quad (5)$$

where r is defined via $r = m_Q/m_Z$. One power of r in Eq. (5) originates from the large momentum transfer that is required for the heavy-quark pair to form the heavy quarkonium with small relative momentum, and the other powers arise from the helicity selection rule in perturbative QCD [24,25].

In terms of the independent helicity amplitudes, the unpolarized decay widths can be explicitly written as

$$\Gamma(Z \to \chi_{Q0} + \gamma) = \frac{1}{3}\frac{1}{2m_Z}\frac{1}{8\pi}\frac{2|\mathbf{P}|}{m_Z}(2|A^{\chi_{Q0}}_{0,1}|^2), \quad (6a)$$

$$\Gamma(Z \to \chi_{Q1} + \gamma) = \frac{1}{3}\frac{1}{2m_Z}\frac{1}{8\pi}\frac{2|\mathbf{P}|}{m_Z}(2|A^{\chi_{Q1}}_{1,1}|^2 + 2|A^{\chi_{Q1}}_{0,1}|^2), \quad (6b)$$

$$\Gamma(Z \to \chi_{Q2} + \gamma) = \frac{1}{3}\frac{1}{2m_Z}\frac{1}{8\pi}\frac{2|\mathbf{P}|}{m_Z} \times (2|A^{\chi_{Q2}}_{2,1}|^2 + 2|A^{\chi_{Q2}}_{1,1}|^2 + 2|A^{\chi_{Q2}}_{0,1}|^2), \quad (6c)$$

$$\Gamma(Z \to h_Q + \gamma) = \frac{1}{3}\frac{1}{2m_Z}\frac{1}{8\pi}\frac{2|\mathbf{P}|}{m_Z}(2|A^{h_Q}_{1,1}|^2 + 2|A^{h_Q}_{0,1}|^2). \quad (6d)$$

The main task of this work remains to compute the helicity amplitudes. The Z boson interacts with the quark-antiquark pair through the tree-level weak interaction as

$$i\mathcal{L}_{ZQ\bar{Q}} = i\frac{g}{4c_W}\bar{Q}\gamma^\mu(g_V - g_A\gamma_5)QZ_\mu, \quad (7)$$

where g is the weak coupling in $SU(2)_L \times U(1)_Y$ electroweak gauge theory, $g_V = 1\text{–}8s_W^2/3$ and $g_A = 1$ for the up-type quark, and $g_V = -1 + 4s_W^2/3$ and $g_A = -1$ for the down-type quark. Here we have defined $s_W \equiv \sin\theta_W$ and $c_W \equiv \cos\theta_W$, where θ_W signifies the Weinberg angle.

The Z boson can decay to $\chi_{QJ} + \gamma$ only through the vectorial interaction, and it can decay to $h_Q + \gamma$ only through the axial-vectorial interaction. Therefore, for simplicity, it is convenient to explicitly extract the electroweak coupling from the helicity amplitudes as

$$A^{\chi_{QJ}}_{\lambda_1,\lambda_2} = \frac{g g_V e e_Q}{4 c_W} \mathcal{A}^{\chi_{QJ}}_{\lambda_1,\lambda_2}, \tag{8a}$$

$$A^{h_Q}_{\lambda_1,\lambda_2} = \frac{g g_A e e_Q}{4 c_W} \mathcal{A}^{h_Q}_{\lambda_1,\lambda_2}. \tag{8b}$$

III. FRAMEWORK OF NRQCD COMPUTATION

A. NRQCD factorization

According to the NRQCD formalism [9], the helicity amplitude $\mathcal{A}^H_{\lambda_1,\lambda_2}$ can be factorized into

$$\mathcal{A}^H_{\lambda_1,\lambda_2} = \sqrt{2m_H} \mathcal{C}^H_{\lambda_1,\lambda_2} \frac{\langle \mathcal{O} \rangle_H}{\sqrt{2N_c} 2m_Q^2}, \tag{9}$$

where $\mathcal{C}^H_{\lambda_1,\lambda_2}$ signify the dimensionless SDCs, $N_c = 3$ is the number of the color, and the NRQCD long-distance matrix elements (LDMEs) are defined via

$$\langle \mathcal{O} \rangle_{\chi_{QJ}} \equiv \langle \chi_{QJ} | \psi^\dagger \mathcal{K}_{^3P_J} \chi | 0 \rangle, \tag{10a}$$

$$\langle \mathcal{O} \rangle_{h_Q} \equiv \langle h_Q | \psi^\dagger \mathcal{K}_{^1P_1} \chi | 0 \rangle, \tag{10b}$$

where $\psi^\dagger$ and χ denote the Pauli spinor fields creating a heavy quark and antiquark in NRQCD, respectively, and

$$\mathcal{K}_{^3P_0} = \frac{1}{\sqrt{3}} \left(-\frac{i}{2} \overleftrightarrow{\mathbf{D}} \cdot \boldsymbol{\sigma} \right), \tag{11a}$$

$$\mathcal{K}_{^3P_1} = \frac{1}{\sqrt{2}} \left(-\frac{i}{2} \overleftrightarrow{\mathbf{D}} \times \boldsymbol{\sigma} \right) \cdot \boldsymbol{\epsilon}_{\chi_{Q1}}, \tag{11b}$$

$$\mathcal{K}_{^3P_2} = -\frac{i}{2} \overleftrightarrow{D}^{(i} \sigma^{j)} \epsilon^{ij}_{\chi_{Q2}}, \tag{11c}$$

$$\mathcal{K}_{^1P_1} = -\frac{i}{2} \overleftrightarrow{\mathbf{D}} \cdot \boldsymbol{\epsilon}_{h_Q}, \tag{11d}$$

with $\epsilon_{\chi_{Q1}}$, ϵ_{h_Q}, and $\epsilon_{\chi_{Q2}}$ representing the polarization vector/tensor of χ_{Q1}, h_Q, and χ_{Q2}, respectively. Exploiting the heavy quark spin symmetry, we can make the following approximations:

$$\langle \mathcal{O} \rangle_{\chi_{Q0}} \approx \langle \mathcal{O} \rangle_{\chi_{Q1}} \approx \langle \mathcal{O} \rangle_{\chi_{Q2}} \approx \langle \mathcal{O} \rangle_{h_Q}. \tag{12}$$

In Eq. (9), the factor $\sqrt{2m_H}$ appears on the right-hand side because we adopt relativistic normalization for the quarkonium H, but we use conventional nonrelativistic normalization for the LDMEs. In this work, we will not compute the relativistic corrections; therefore, it is reasonable to take the approximation $m_H \approx 2m_Q$.

Through Eqs. (5) and (9), we can readily deduce the helicity selection rule for the SDCs

$$\mathcal{C}^H_{\lambda_1,\lambda_2} \propto r^{|\lambda_1|} \tag{13}$$

by noting that $\langle \mathcal{O} \rangle_H \propto m_Q^{5/2}$.

The SDCs are insensitive to the nonperturbative hadronization effects; therefore, they can be determined with the aid of the standard perturbative matching technique. That is, by replacing the physical H meson with a fictitious onium composed of a free $Q\bar{Q}$ pair, carrying the quantum number ^3P_J for χ_{QJ} and $^1P_1$ for h_Q, we compute both sides of Eq. (9). After that, we are able to solve for the desired SDCs. For more details, we refer the readers to Ref. [26].

It is convenient to parametrize the SDCs in powers of α_s,

$$\mathcal{C}^H_{\lambda_1,\lambda_2} = \mathcal{C}^{H,(0)}_{\lambda_1,\lambda_2} \left[1 + \frac{\alpha_s}{\pi} \mathcal{C}^{H,(1)}_{\lambda_1,\lambda_2} + \frac{\alpha_s^2}{\pi^2} \left(\frac{\beta_0}{4} \ln \frac{\mu_R^2}{m_Q^2} \mathcal{C}^{H,(1)}_{\lambda_1,\lambda_2} + \gamma_H \ln \frac{\mu_\Lambda}{m_Q} + \mathcal{C}^{H,(2)}_{\mathrm{reg},\lambda_1,\lambda_2} + \mathcal{C}^{H,(2)}_{\mathrm{nonreg},\lambda_1,\lambda_2} \right) \right] + \mathcal{O}(\alpha_s^3), \tag{14}$$

where μ_R and μ_Λ signify the renormalization scale and factorization scale, respectively, and $\beta_0 = (11/3)C_A - (4/3)T_F n_f$ is the one-loop coefficient of the QCD β function, where n_f is the number of active quark flavors. The explicit $\ln \mu_R^2$ term is deduced from the renormalization-group invariance. γ_H represent the anomalous dimensions associated with the NRQCD bilinear currents carrying the quantum numbers ^3P_J or $^1P_1$, the expressions of which read [27]

$$\gamma_{^3P_0} = -\pi^2 \left(\frac{C_A C_F}{6} + \frac{2C_F^2}{3} \right), \tag{15a}$$

$$\gamma_{^3P_1} = -\pi^2 \left(\frac{C_A C_F}{6} + \frac{5C_F^2}{12} \right), \tag{15b}$$

$$\gamma_{^3P_2} = -\pi^2 \left(\frac{C_A C_F}{6} + \frac{13C_F^2}{60} \right), \tag{15c}$$

$$\gamma_{^1P_1} = -\pi^2 \left(\frac{C_A C_F}{6} + \frac{C_F^2}{3} \right). \tag{15d}$$

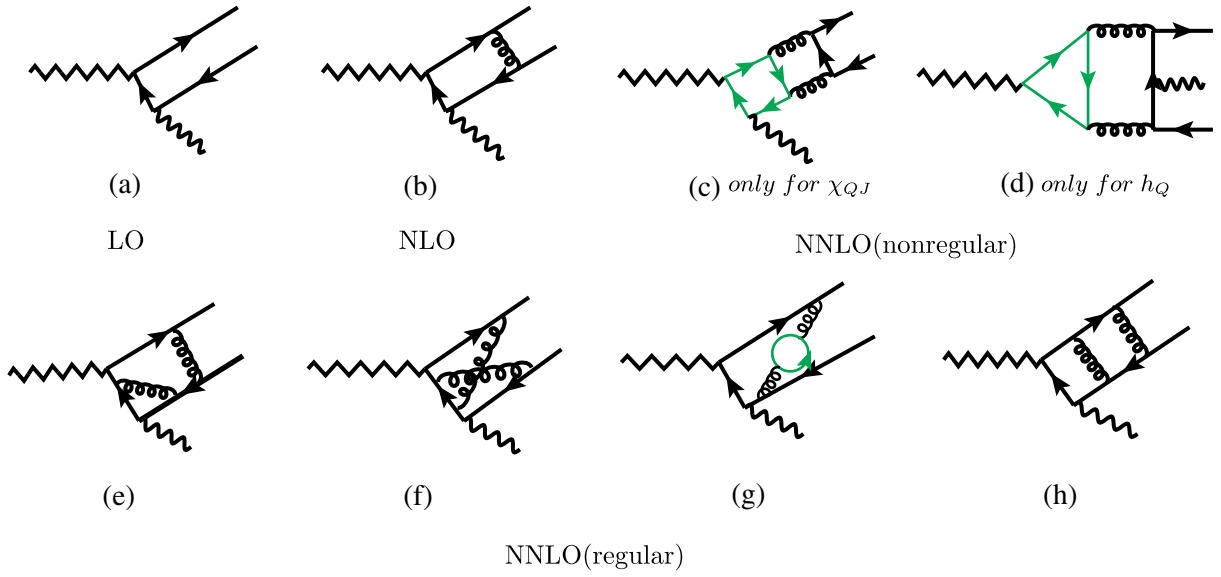

FIG. 1. Some representative Feynman diagrams for the process $Z \to \chi_{QJ}(h_Q) + \gamma$ up to $\mathcal{O}(\alpha_s^2)$.

The occurrence of $\ln \mu_\Lambda$ is required by the NRQCD factorization. According to the factorization, the μ_Λ dependence in the SDCs should be thoroughly canceled by that in the LDMEs. As illustrated in Fig. 1, we classify the Feynman diagrams into a "regular" part and a "nonregular" part at $\mathcal{O}(\alpha_s^2)$. Correspondingly, $\mathcal{C}^{H,(2)}_{\mathrm{reg},\lambda_1,\lambda_2}$ and $\mathcal{C}^{H,(2)}_{\mathrm{nonreg},\lambda_1,\lambda_2}$ in Eq. (14) represent contributions from the regular Feynman diagrams and the nonregular Feynman diagrams, respectively.

B. SDCs through $\mathcal{O}(\alpha_s^2)$

The quark-level Feynman diagrams and Feynman amplitudes are generated using FeynArts [28]. Employing the color and spin projectors followed by enforcing spin-orbit coupling, we obtain the hadron-level amplitudes order by order in α_s with the aid of the packages FeynCalc [29] and FormLink [30]. To evaluate the helicity amplitudes, we employ the technique of helicity projection. The concrete expressions of all the helicity projectors are presented in Appendix.

It is well known that, in dimensional regularization, the anticommutation relation $\{\gamma^\mu, \gamma_5\}$ and the cyclicity of Dirac trace cannot be satisfied simultaneously. In practical computation, the naive-γ_5 scheme [31], which keeps the anticommutation relation $\{\gamma^\mu, \gamma_5\}$, is frequently applied. In this scheme, spurious anomaly, which spoils chiral symmetry and hence gauge invariance, can be avoided. Because of the lack of the cyclicity of the trace, one must fix a reading point for a fermion loop with an odd number of γ_5. In our work, we will select the vertex of the Z boson as the reading point.

Then, it is straightforward to obtain the LO helicity SDCs:

$$\mathcal{C}^{\chi_{Q0},(0)}_{0,1} = \frac{2\sqrt{2}(1-12r^2)}{1-4r^2}, \tag{16a}$$

$$\mathcal{C}^{\chi_{Q1},(0)}_{1,1} = -\frac{8\sqrt{3}r}{1-4r^2}, \qquad \mathcal{C}^{\chi_{Q1},(0)}_{0,1} = \frac{4\sqrt{3}}{1-4r^2}, \tag{16b}$$

$$\mathcal{C}^{\chi_{Q2},(0)}_{2,1} = -\frac{16\sqrt{6}r^2}{1-4r^2}, \qquad \mathcal{C}^{\chi_{Q2},(0)}_{1,1} = \frac{8\sqrt{3}r}{1-4r^2},$$
$$\mathcal{C}^{\chi_{Q2},(0)}_{0,1} = -\frac{4}{1-4r^2}, \tag{16c}$$

$$\mathcal{C}^{h_Q,(0)}_{1,1} = 4\sqrt{6}r, \qquad \mathcal{C}^{h_Q,(0)}_{0,1} = -2\sqrt{6}. \tag{16d}$$

Once beyond the LO, we adopt the standard shortcut to directly extract the SDCs, i.e., compute the hard region in the context of the strategy of the region [32]. Utilizing the packages APART [33] and FIRE [34], we can further reduce the loop integrals into linear combinations of master integrals (MIs). Finally, we end up with 6 one-loop MIs, which are computed using PACKAGE-X [35], and roughly 320 two-loop MIs, the evaluation of which is a challenging work. Fortunately, a powerful new algorithm, dubbed auxiliary mass flow (AMF), has recently been pioneered by Liu and Ma [36–38]. Its main idea is to set up differential equations with respect to an auxiliary mass variable, with the vacuum bubble diagrams as the boundary conditions. Remarkably, these differential equations can be solved iteratively with very high numerical precision. In this work, we utilize the newly released package AMFlow [39] to compute all the two-loop MIs. After implementing the on-shell renormalization scheme for the heavy quark mass and field strength [40], and the $\overline{\mathrm{MS}}$ renormalization scheme for the QCD coupling, the UV poles are exactly canceled, while an uncanceled single IR pole still remains.

TABLE I. NRQCD predictions to the various helicity SDCs defined in Eq. (14) for charmonium production. For simplicity, we define the symbols $f_1 \equiv \frac{g_V^d}{g_V^u} = -\frac{3-4S_W^2}{3-8S_W^2}$ and $f_2 \equiv \frac{g_V^u - g_V^d}{g_V^u} = \frac{6-12S_W^2}{3-8S_W^2}$, where g_V^u and g_V^d correspond to the values of g_V for the up-type quark and the down-type quark, respectively.

H	(λ_1,λ_2)	$\mathcal{C}^{(1)}_{\lambda_1,\lambda_2}$	$\mathcal{C}^{(2)}_{\mathrm{reg},\lambda_1,\lambda_2}$	$\mathcal{C}^{(2)}_{\mathrm{nonreg},\lambda_1,\lambda_2}$
χ_{c0}	(0,1)	$0.09+0.43i$	$-2.00-2.21i-(2.34-1.29i)n_l$ $-(1.12-1.28i)n_c-(0.58-1.25i)n_b$	$(6.43-7.29i)n_c-(1.57-3.71i)f_1n_b$ $+(9.49-6.37i)f_2$
χ_{c1}	(1,1)	$1.11-1.69i$	$-29.65+22.87i-(0.32+0.92i)n_l$ $-(0.09+0.92i)n_c-(0.03+0.93i)n_b$	$-(3.01-1.60i)n_c+(0.72-0.78i)f_1n_b$ $-(3.43+0.04i)f_2$
	(0,1)	$0.77-1.68i$	$-28.51+24.13i-(0.53+0.74i)n_l$ $-(0.29+0.74i)n_c-(0.23+0.76i)n_b$	$-(3.67-2.73i)n_c+(0.77-1.30i)f_1n_b$ $-(4.66-0.89i)f_2$
χ_{c2}	(2,1)	$-6.83+1.62i$	$240.12-37.67i+(0.06+1.67i)n_l$ $-(1.45-1.67i)n_c-(2.93-1.68i)n_b$	$(181.76-21.31i)n_c-(88.77-40.30i)f_1n_b$ $+(173.42-2.68i)f_2$
	(1,1)	$-8.44+2.50i$	$10.19-53.70i-(0.22-2.43i)n_l$ $-(1.84-2.43i)n_c-(3.52-2.43i)n_b$	$(3.35-0.65i)n_c-(1.59-0.79i)f_1n_b$ $+(3.37-0.29i)f_2$
	(0,1)	$-4.69+0.43i$	$-6.96-8.92i-(0.84-1.30i)n_l$ $-(1.60-1.29i)n_c-(2.40-1.25i)n_b$	$(5.23-2.15i)n_c-(1.89-1.85i)f_1n_b$ $+(5.10-1.31)f_2$
h_c	(1,1)	$-8.39+2.89i$	$10.52-64.86i-(0.54-2.62i)n_l$ $-(1.85-2.63i)n_c-(3.46-2.64i)n_b$	$1.66+1.62i$
	(0,1)	$-4.01+0.43i$	$-(9.98+7.77i)-(1.20-1.29i)n_l$ $-(1.57-1.29i)n_c-(2.15-1.25i)n_b$	$1.75+1.56i$

This symptom is a common feature specific to the NRQCD factorization, which has been encountered many times in NNLO perturbative calculations involving quarkonium. This IR pole can be factored into the NRQCD LDME, so that the NRQCD SDCs become IR finite. We have numerically verified that the coefficient of the remaining IR pole is equal to one-quarter of the anomalous dimension in Eq. (15) with high precision, as required by the NRQCD factorization.

The analytic expressions of $\mathcal{C}^{H,(1)}_{\lambda_1,\lambda_2}$ can readily be obtained. Instead of presenting the cumbersome expressions, here we merely present their asymptotic expansions in $r \to 0$:

$$\mathcal{C}^{\chi_{Q0},(1)}_{0,1} = \frac{1}{3}(2\ln 2-1)\ln(-r^2+i\epsilon)+\frac{\ln^2 2}{3}+3\ln 2-\frac{\pi^2}{9}, \tag{17a}$$

$$\mathcal{C}^{\chi_{Q1},(1)}_{1,1} = \frac{1}{3}(2\ln 2-3)\ln(-r^2+i\epsilon)+\frac{\ln^2 2}{3}-\frac{\ln 2}{3}-\frac{\pi^2}{9}-2, \tag{17b}$$

$$\mathcal{C}^{\chi_{Q1},(1)}_{0,1} = \frac{1}{3}(2\ln 2-3)\ln(-r^2+i\epsilon)+\frac{\ln^2 2}{3}-\frac{\ln 2}{3}-\frac{\pi^2}{9}-\frac{7}{3}, \tag{17c}$$

$$\mathcal{C}^{\chi_{Q2},(1)}_{2,1} = \frac{4}{3}(2\ln 2-1)\ln(-r^2+i\epsilon)+\frac{4\ln^2 2}{3}+\frac{16\ln 2}{3}-\frac{4\pi^2}{9}-\frac{8}{3}, \tag{17d}$$

$$\mathcal{C}^{\chi_{Q2},(1)}_{1,1} = \frac{1}{3}(2\ln 2+1)\ln(-r^2+i\epsilon)+\frac{\ln^2 2}{3}-\frac{5\ln 2}{3}-\frac{\pi^2}{9}, \tag{17e}$$

$$\mathcal{C}^{\chi_{Q2},(1)}_{0,1} = \frac{1}{3}(2\ln 2-1)\ln(-r^2+i\epsilon)+\frac{\ln^2 2}{3}-\ln 2-\frac{\pi^2}{9}-2, \tag{17f}$$

$$\mathcal{C}^{h_Q,(1)}_{1,1} = \frac{4}{3}\ln 2\ln(-r^2+i\epsilon)+\frac{2\ln^2 2}{3}+\frac{8\ln 2}{3}-\frac{2\pi^2}{9}-1, \tag{17g}$$

$$\mathcal{C}^{h_Q,(1)}_{0,1} = \frac{1}{3}(2\ln 2-1)\ln(-r^2+i\epsilon)+\frac{\ln^2 2}{3}-\ln 2-\frac{\pi^2}{9}-\frac{4}{3}, \tag{17h}$$

where the real parts of the results in Eqs. (17a)–(17f) are consistent with those in Ref. [41],[1] and the results in Eqs. (17a), (17c), (17f), and (17h) are consistent with those in Ref. [12].

It is rather challenging for us to analytically compute $\mathcal{C}^{H,(2)}_{\lambda_1,\lambda_2}$, so we turn to numerically evaluate their values. To perform the numerical computation, we take $m_Z = 91.1876$ GeV from the latest Particle Data Group (PDG) [42], and the pole masses of the charm quark and bottom quark to be $m_c = 1.69$ GeV and $m_b = 4.80$ GeV, which are converted from the $\overline{\mathrm{MS}}$ masses $\bar{m}_c(\bar{m}_c) = 1.28$ GeV

[1]In Ref. [41], only the cross sections of $e^+e^- \to \chi_{cJ}+\gamma$ are presented, where the imaginary parts of the amplitudes are ignored.

TABLE II. NRQCD predictions to the various helicity SDCs for bottomonium production. For simplicity, we define the symbols $\bar{f}_1 \equiv \frac{g_V^u}{g_V^d} = -\frac{3-8S_W^2}{3-4S_W^2}$, $\bar{f}_2 \equiv \frac{2g_V^d-2g_V^u}{g_V^d} = \frac{12-24S_W^2}{3-4S_W^2}$.

H	(λ_1,λ_2)	$\mathcal{C}^{(1)}_{\lambda_1,\lambda_2}$	$\mathcal{C}^{(2)}_{\mathrm{reg},\lambda_1,\lambda_2}$	$\mathcal{C}^{(2)}_{\mathrm{nonreg},\lambda_1,\lambda_2}$
χ_{b0}	(0,1)	$0.35+0.58i$	$-4.41-6.16i-(1.47-1.15i)n_l$ $-(0.35-1.14i)n_c-(0.22-1.10i)n_b$	$-(8.02-11.05i)\bar{f}_1 n_c+(1.83-5.06i)n_b$ $+(5.06-4.40i)\bar{f}_2$
χ_{b1}	(1,1)	$-0.07-1.65i$	$-18.06+10.67i-(0.75+0.28i)n_l$ $-(0.17+0.28i)n_c-(0.50+0.29i)n_b$	$+(4.83-0.96i)\bar{f}_1 n_c-(1.81-1.75i)n_b$ $-(2.28-0.14i)\bar{f}_2$
	(0,1)	$-0.42-1.61i$	$-16.52+10.33i-(0.83+0.10i)n_l$ $-(0.25+0.10i)n_c-(0.57+0.13i)n_b$	$+(5.54-2.50i)\bar{f}_1 n_c-(1.76-2.47i)n_b$ $-(2.85-0.75i)\bar{f}_2$
χ_{b2}	(2,1)	$-5.77+1.63i$	$8.69-27.65i+(0.98+1.12i)n_l$ $+(0.72+1.12i)n_c-(0.54-1.13i)n_b$	$-(47.72-8.15i)\bar{f}_1 n_c+(23.15-11.58i)n_b$ $+(22.90-1.73i)\bar{f}_2$
	(1,1)	$-6.77+2.50i$	$-20.19-37.37i+(1.11+1.55i)n_l$ $+(0.83+1.55i)n_c-(0.51-1.55i)n_b$	$-(3.88-0.97i)\bar{f}_1 n_c+(1.88-0.71i)n_b$ $+(1.89-0.23i)\bar{f}_2$
	(0,1)	$-4.50+0.57i$	$-13.91-13.04i+(0.02+1.20i)n_l$ $+(0.11+1.19i)n_c-(0.73-1.15i)n_b$	$-(4.56-1.86i)\bar{f}_1 n_c+(2.20-1.47i)n_b$ $+(2.14-0.70)\bar{f}_2$
h_b	(1,1)	$-6.43+2.85i$	$-(25.69+42.26i)+(0.87+1.59i)n_l$ $+(0.78+1.59i)n_c-(0.45-1.60i)n_b$	$-1.71-1.60i$
	(0,1)	$-3.78+0.54i$	$-(16.35+11.34i)-(0.35-1.17i)n_l$ $-(0.03-1.17i)n_c-(0.69-1.13i)n_b$	$-1.76-1.54i$

and $\bar{m}_b(\bar{m}_b) = 4.18$ GeV [42] at the two-loop level by the use of the package RunDec [43].

We tabulate the results of the SDCs $\mathcal{C}^{H,(1)}_{\lambda_1,\lambda_2}$, $\mathcal{C}^{H,(2)}_{\mathrm{reg},\lambda_1,\lambda_2}$, and $\mathcal{C}^{H,(2)}_{\mathrm{nonreg},\lambda_1,\lambda_2}$ in Table I for charmonium production and in Table II for bottomonium production.[2] For the sake of reference, we explicitly keep the n_l, n_c, and n_b dependence in the SDCs, where n_l denotes the number of the light quarks, and $n_c = 1$ and $n_b = 1$ signify the numbers of the charm quark and bottom quark, respectively.

IV. LC FACTORIZATION FOR THE LEADING-TWIST SDCS

A. The LC factorization

Besides the NRQCD factorization formalism, we can also employ the LC factorization framework to calculate the decay amplitude for $Z \to H + \gamma$ at the leading twist. By following the spirit of Ref. [20], the LC factorization formula for the SDCs is written as

$$\mathcal{C}^H_{0,1}(\mu; m_Z, m_Q) = \mathcal{C}^{H,\mathrm{LL}_0}_{0,1} \int_0^1 dx T_H(x,\mu)\hat{\phi}_H(x,\mu) + \mathcal{O}(r^2), \tag{18}$$

where $\mathcal{C}^{H,\mathrm{LL}_0}_{0,1}$ represents the asymptotic expansion of $\mathcal{C}^{H,(0)}_{0,1}$ in $r \to 0$, and the hard-kernel T_H and the leading-twist LC distribution amplitude (LCDA) $\hat{\phi}_H$ are perturbatively calculable around the scale m_Z and m_Q, respectively. At LO in α_s, we have

$$T_H(x,\mu = m_Z) = T_H^{(0)}(x) = \begin{cases} \frac{1}{4}(\frac{1}{1-x}-\frac{1}{x}), & \text{for } H = h_Q, \chi_{Q0} \text{ and } \chi_{Q2}, \\ \frac{1}{4}(\frac{1}{1-x}+\frac{1}{x}), & \text{for } H = \chi_{Q1}, \end{cases} \tag{19}$$

$$\hat{\phi}_H(x,\mu = m_Q) = \hat{\phi}_H^{(0)}(x) = \begin{cases} -\frac{1}{2}\delta'(x-1/2), & \text{for } H = h_Q, \chi_{Q0} \text{ and } \chi_{Q2}, \\ \delta(x-1/2), & \text{for } H = \chi_{Q1}. \end{cases} \tag{20}$$

We can reproduce the asymptotic expansions of the SDCs $\mathcal{C}^{H,(1)}_{0,1}$ in Eq. (17) exactly with the corresponding NLO corrections to T_H and $\hat{\phi}_H$ that have been calculated in [12]. More importantly, we can employ the LC factorization to resum the LL terms $(\alpha_s \ln r^2)^n$ in $\mathcal{C}^H_{0,1}$.

B. Resummation of the LL with the ERBL equation

The leading twist LCDAs $\hat{\phi}_H$ obey the celebrated ERBL equation [21,44]

$$\mu^2 \frac{d}{d\mu^2}\hat{\phi}_H(x;\mu) = \frac{\alpha_s(\mu)}{2\pi} C_F \int_0^1 V(x,y)\hat{\phi}_H(y;\mu), \tag{21}$$

with the Brodsky-Lepage (BL) kernel

[2]Since weak interaction in the Standard Model (SM) is a chiral gauge theory, the gauge anomaly should be avoided for physical processes. To satisfy the condition of anomaly free, when evaluating $\mathcal{C}^{h_Q,(2)}_{\mathrm{nonreg},\lambda_1,\lambda_2}$, which corresponds to the contribution from Fig. 1(d), we have included all six flavor quark loops.

$$V(x,y)=\left[\frac{1-x}{1-y}\left(1+\frac{1}{x-y}\right)\theta(x-y)+\frac{x}{y}\left(1+\frac{1}{y-x}\right)\theta(y-x)\right]_+, \tag{22}$$

where the subscript "+" implies the familiar "plus" prescription.

Solving the ERBL equation, we can obtain the SDCs with all the LL terms $(\alpha_s \ln r^2)^n$ resummed. Formally, we have

$$\mathcal{C}_{0,1}^{H,\mathrm{LL}}=\mathcal{C}_{0,1}^{H,\mathrm{LL}_0}\mathcal{K}_H^{\mathrm{LL}}, \tag{23}$$

with

$$\mathcal{K}_H^{\mathrm{LL}}=\int_0^1 dx T^{H,(0)}(x)\exp(\kappa C_F V\star)\hat{\phi}_H^{(0)}(x), \tag{24}$$

where

$$\kappa\equiv\frac{2}{\beta_0}\ln\left(\frac{\alpha_s(m_Q)}{\alpha_s(m_Z)}\right)=-\frac{\alpha_s(m_Z)}{2\pi}\ln r^2+\beta_0\frac{\alpha_s^2(m_Z)}{(4\pi)^2}\ln^2 r^2+\cdots, \tag{25}$$

with "$\star$" standing for the convolution

$$[V\star\hat{\phi}](x)\equiv\int_0^1 dy V(x,y)\hat{\phi}(y). \tag{26}$$

It is well known that the BL kernel has the eigensystem that

$$\int_0^1 V(x,y)G_n(y)=-\gamma_n G_n(x), \tag{27}$$

where

$$\gamma_n=\frac{1}{2}+2\sum_{j=2}^{n+1}\frac{1}{j}-\frac{1}{(n+1)(n+2)}, \tag{28}$$

and the eigenfunctions

$$G_n(x)\equiv x(1-x)C_n^{(3/2)}(2x-1), \tag{29}$$

with $C_n^{(3/2)}(2x-1)$ being order 3/2 Gegenbauer polynomials. We can decompose the LCDA $\hat{\phi}_H^{(0)}(x)$ in the basis of G_n:

$$\hat{\phi}_H^{(0)}(x)=\sum_{n=0}^{\infty}\hat{\phi}_{H,n}^{(0)}G_n(x), \tag{30}$$

where

$$\hat{\phi}_{H,n}^{(0)}=\frac{4(2n+3)}{(n+1)(n+2)}\int_0^1 dx C_n^{(3/2)}(2x-1)\hat{\phi}_H^{(0)}(x). \tag{31}$$

Hence, we can get

$$\exp(\kappa C_F V\star)\hat{\phi}_H^{(0)}(x)=\sum_{n=0}^{\infty}\hat{\phi}_{H,n}^{(0)}\left(\frac{\alpha_s(m_Q)}{\alpha_s(m_Z)}\right)^{-2\gamma_n C_F/\beta_0}G_n(x). \tag{32}$$

Employing

$$\int_0^1 dx\frac{1}{x}G_n(x)=(-1)^n\frac{1}{2}, \tag{33}$$

and the decompositions

$$\delta(x-1/2)=\sum_{n=0}^{\infty}\frac{2(4n+3)}{(2n+1)(n+1)}(-1)^n\frac{(2n+1)!!}{(2n)!!}G_{2n}(x), \tag{34a}$$

$$-\frac{1}{2}\delta'(x-1/2)=\sum_{n=0}^{\infty}\frac{2(4n+5)}{(n+1)(2n+3)}\times(-1)^n\frac{(2n+3)!!}{(2n)!!}G_{2n+1}(x), \tag{34b}$$

we get

$$\mathcal{K}_H^{\mathrm{LL}}=\frac{1}{4}\sum_{n=0}^{\infty}\frac{2(4n+3)}{(2n+1)(n+1)}\times(-1)^n\frac{(2n+1)!!}{(2n)!!}\left(\frac{\alpha_s(m_Z)}{\alpha_s(m_Q)}\right)^{2C_F\gamma_{2n}/\beta_0}, \tag{35}$$

for $H=\chi_{Q1}$, and

$$\mathcal{K}_H^{\mathrm{LL}}=\frac{1}{4}\sum_{n=0}^{\infty}\frac{2(4n+5)}{(2n+3)(n+1)}\times(-1)^n\frac{(2n+3)!!}{(2n)!!}\left(\frac{\alpha_s(m_Z)}{\alpha_s(m_Q)}\right)^{2C_F\gamma_{2n+1}/\beta_0}, \tag{36}$$

for $H=\chi_{Q0},\chi_{Q2}$, and h_Q.

With the explicit expansion of the formal solution in Eq. (24) in κ and the formulas

$$\int_0^1 dy\frac{1}{y}V(y,x)=\frac{1}{x}\left[\frac{3}{2}+\ln x\right], \tag{37a}$$

$$\int_0^1 dz\int_0^1 dy\frac{1}{z}V(z,y)V(y,x)=\frac{1}{x}\left[\frac{9}{4}+\frac{3-2x}{1-x}\ln x+\ln^2 x+\mathrm{Li}_2(1-x)-\frac{\pi^2}{6}\right], \tag{37b}$$

we can obtain the expansion of $\mathcal{K}_H^{\rm LL}$ in α_s,

$$\mathcal{K}_H^{\rm LL} = 1 - \frac{\alpha_s(m_Z)}{4\pi} C_F \ln r^2 [3 - 2\ln 2] + \frac{\alpha_s^2(m_Z)}{(4\pi)^2} \ln^2 r^2 \left[C_F^2 \left(\frac{9}{2} - 8\ln 2 + \ln^2 2 - \frac{\pi^2}{6} \right) + C_F \beta_0 \left(\frac{3}{2} - \ln 2 \right) \right] + \mathcal{O}(\alpha_s^3), \tag{38}$$

for $H = \chi_{Q1}$, and

$$\mathcal{K}_H^{\rm LL} = 1 - \frac{\alpha_s(m_Z)}{4\pi} C_F \ln r^2 [1 - 2\ln 2] + \frac{\alpha_s^2(m_Z)}{(4\pi)^2} \ln^2 r^2 \left[C_F^2 \left(-\frac{7}{2} + 2\ln 2 + \ln^2 2 - \frac{\pi^2}{6} \right) + C_F \beta_0 \left(\frac{1}{2} - \ln 2 \right) \right] + \mathcal{O}(\alpha_s^3), \tag{39}$$

for $H = \chi_{Q0}, \chi_{Q2}$, and h_Q.

C. SDCs by combining the fixed-order results and the LL resummation

In the following, we will improve the leading-twist SDCs by combining the NRQCD fixed-order results given in Sec. III and the LL resummation sketched in Sec. IV A and Sec. IV B.

To avoid double counting, it is necessary to subtract the terms of $\mathcal{O}(\alpha_s^n \ln^n r)$ from the fixed-order SDCs. Formally, we have

$$\mathcal{C}_{0,1}^{H,\rm LO+LL} = \mathcal{C}_{0,1}^{H,\rm LO} - \mathcal{C}_{0,1}^{H,\rm LL_0} + \mathcal{C}_{0,1}^{H,\rm LL}, \tag{40a}$$

$$\mathcal{C}_{0,1}^{H,\rm NLO+LL} = \mathcal{C}_{0,1}^{H,\rm NLO} - \mathcal{C}_{0,1}^{H,\rm LL_1} + \mathcal{C}_{0,1}^{H,\rm LL}, \tag{40b}$$

$$\mathcal{C}_{0,1}^{H,\rm NNLO+LL} = \mathcal{C}_{0,1}^{H,\rm NNLO} - \mathcal{C}_{0,1}^{H,\rm LL_2} + \mathcal{C}_{0,1}^{H,\rm LL}, \tag{40c}$$

where the superscripts "LO," "NLO," and "NNLO" denote the fixed-order SDCs accurate up to $\mathcal{O}(\alpha_s^0)$, $\mathcal{O}(\alpha_s^1)$, and $\mathcal{O}(\alpha_s^2)$, respectively, and the superscripts "$\rm LL_0$," "$\rm LL_1$," and "$\rm LL_2$" signify the $\mathcal{C}_{0,1}^{H,\rm LL}$ truncated at $\mathcal{O}(\alpha_s^0)$, $\mathcal{O}(\alpha_s^1)$, and $\mathcal{O}(\alpha_s^2)$, respectively, which have been explicitly computed in Sec. IV B.

In Table III, we present the theoretical predictions on the squared leading-twist SDCs $|\mathcal{C}_{0,1}^H|^2$ at various levels of accuracy. In the table, we also enumerate the values of $\mathcal{K}_H^{\rm LL}$, which are computed by applying Eqs. (35) and (36) with $\alpha_s(m_Z) = 0.1181$, taken from the PDG, and $\alpha_s(m_c) = 0.3240$ and $\alpha_s(m_b) = 0.2151$, evaluated through the renormalization group running at two-loop with the aid of the package RunDec. It is worth noting that, in order to accelerate the convergence, we have used the so-called Abel-Padé method [45] to sum the series in Eqs. (35) and (36).

From Table III, we have several observations. First, we find the fixed-order predictions for charmonium production are close to these for bottomonium production; however, the LL resummation can give rise to some differences. Second, we notice that the effect of the LL resummation can considerably change the LO results, especially for charmonium production, for instance, it can change the LO results by more than 25% for $\chi_{c0,2}$ and h_c production, and by around 50% for χ_{c1} production. The magnitude of the LL resummation for bottomium production is roughly half of that for charmonium case. Finally, it is worth noting that the effects of the LL resummation on the NLO and NNLO predictions are continuously becoming milder. It can be explained by the fact that some of the LL resummations have been included in the radiative corrections. Concretely, the $\mathcal{O}(\alpha_s \ln r)$ contribution has been included in the NLO prediction, while both the $\mathcal{O}(\alpha_s \ln r)$ and the $\mathcal{O}(\alpha_s^2 \ln^2 r)$ contributions have been included in the NNLO prediction. As a consequence, the remaining contribution from the LL resummation can correspondingly reduce its effect on the NLO and NNLO predictions.

V. PHENOMENOLOGY

To make concrete phenomenological predictions, we need to fix the various input parameters. We take $m_Z = 91.1876$ GeV from PDG, and the heavy quark pole masses $m_c = 1.69$ GeV and $m_b = 4.80$ GeV, as mentioned, which are converted from their $\overline{\rm MS}$ masses. We take the running QED coupling constant evaluated at the mass of m_Z as

TABLE III. Squared leading-twist SDCs $|\mathcal{C}_{0,1}^H|^2$ at various levels of accuracy. We take $\mu_R = m_Z$ and $\mu_\Lambda = 1$ GeV.

H	$\mathcal{K}_H^{\rm LL}$	LO	LO + LL	NLO	NLO + LL	NNLO	NNLO + LL
χ_{c0}	0.859	7.96	5.87	8.01	6.47	8.85	7.90
χ_{c1}	1.222	48.13	71.88	51.15	57.38	47.07	50.63
χ_{c2}	0.859	16.04	11.86	10.89	8.37	8.87	7.54
h_c	0.859	24.00	17.73	17.31	13.41	13.51	11.50
χ_{b0}	0.930	7.65	6.59	7.85	7.21	8.87	8.58
χ_{b1}	1.145	49.08	64.25	47.72	50.31	45.52	46.78
χ_{b2}	0.930	16.36	14.18	11.30	10.23	9.90	9.47
h_b	0.930	24.00	20.77	17.68	16.02	15.26	14.61

$\alpha(m_Z) = 1/128.943$ [46]. We take the NRQCD factorization scale $\mu_\Lambda = 1$ GeV. The NRQCD LDMEs for χ_{QJ} and h_Q are approximated by the first derivative of the Schrödinger radial wave function at origin through

$$|\langle\mathcal{O}\rangle_{\chi_{cJ}}|^2 \approx |\langle\mathcal{O}\rangle_{h_c}|^2 \approx \frac{3N_c}{2\pi}|R'_{1P,c\bar{c}}(0)|^2 = \frac{3N_c}{2\pi} \times 0.075\ \text{GeV}^5, \tag{41a}$$

$$|\langle\mathcal{O}\rangle_{\chi_{bJ}}|^2 \approx |\langle\mathcal{O}\rangle_{h_b}|^2 \approx \frac{3N_c}{2\pi}|R'_{1P,b\bar{b}}(0)|^2 = \frac{3N_c}{2\pi} \times 1.417\ \text{GeV}^5, \tag{41b}$$

where the $1P$ radial wave functions at origin, evaluated in the Buchmüller-Tye (BT) potential model, are taken from Ref. [47]. In addition, we take $s_W^2 = 0.231$, and the value of the total decay width of the Z boson $\Gamma_Z = 2.4952$ GeV from the PDG [42].

With all ingredients in hand, we can compute the decay widths of $Z \to H + \gamma$. The unpolarized decay widths at various levels of accuracy for charmonium production and bottomonium production are separately tabulated in Tables IV and V. In the tables, we have included the uncertainties from the ambiguity of the renormalization scale and QCD higher-order corrections. We should emphasize that the values of the Schrödinger wave functions may largely affect the theoretical predictions on the decay rates; i.e., $|R'_{1P,c\bar{c}}(0)|^2$ can range from 0.07 to 0.13 GeV^5, and $|R'_{1P,b\bar{b}}(0)|^2$ can range from 0.93 to 2.07 GeV^5 in Refs. [47,48], which may change the central values of the decay rates of quarkonium production by roughly a factor of 2.

It is interesting to note that both the $\mathcal{O}(\alpha_s)$ and the $\mathcal{O}(\alpha_s^2)$ corrections to $Z \to \chi_{Q2}/h_Q + \gamma$ are sizable and negative. The LL resummation turns out to further decrease the decay widths. Incorporating all the perturbative corrections and LL resummation reduces the LO prediction by roughly half of the magnitude. In contrast, both the $\mathcal{O}(\alpha_s)$ and the $\mathcal{O}(\alpha_s^2)$ corrections are moderate or even minor for other channels. The situation is quite similar to the case in Ref. [26], where the radiative corrections are significant for $e^+e^- \to \chi_{c2} + \gamma$ at B factory, however inconsiderable for $e^+e^- \to \chi_{c0,1} + \gamma$.

It is enlightening to compare the strengths of the decay widths for different quarkonium production. For charmonium production, we find that $h_c + \gamma$ production has the biggest branching fraction, followed by $\chi_{c1} + \gamma$ production. Although the branching fraction of $\chi_{c2} + \gamma$ is 2 times larger than that of $\chi_{c0} + \gamma$ at LO, their branching fractions are nearly the same at NNLO + LL accuracy. For bottomonium production, we notice that the branching fractions of $\chi_{b1} + \gamma$, $h_b + \gamma$, $\chi_{c2} + \gamma$, and $\chi_{b0} + \gamma$ make the most, second, third, and last strengths.

It is worth noting that, for the same quantum number of quarkonium, the branching fraction of charmonium production is larger than that of bottomium production. Finally, we estimate the number of the quarkonium production at the proposed super Z factories, such as the Z-factory mode in CEPC, where the Z boson yield will reach 7×10^{11} [6]. Thus it is expected that there will be

TABLE IV. Unpolarized (total) decay widths for $Z \to$ charmonium $+ \gamma$ at various levels of accuracy. The predictions are obtained by setting $\mu_R = m_Z/\sqrt{2}$. The first error at accuracy of NNLO and NNLO + LL is estimated by varying μ_R from $m_Z/2$ to m_Z, while the second error is from the QCD higher-order corrections, which are estimated through $\alpha_s^3 \sim 0.002$.

Channel	Order	Γ_{total}(eV)	Br($\times 10^{-9}$)
$Z \to \chi_{c0} + \gamma$	LO	0.939	0.376
	NLO	0.946	0.379
	NNLO	$1.056^{+0.014+0.002}_{-0.012-0.002}$	$0.423^{+0.006+0.001}_{-0.005-0.001}$
	NNLO + LL	$0.944^{+0.013+0.002}_{-0.011-0.002}$	$0.374^{+0.005+0.001}_{-0.005-0.001}$
$Z \to \chi_{c1} + \gamma$	LO	5.687	2.279
	NLO	6.066	2.431
	NNLO	$5.529^{+0.033+0.011}_{-0.040-0.011}$	$2.216^{+0.013+0.004}_{-0.016-0.004}$
	NNLO + LL	$5.947^{+0.035+0.011}_{-0.042-0.011}$	$2.383^{+0.014+0.004}_{-0.017-0.004}$
$Z \to \chi_{c2} + \gamma$	LO	1.901	0.762
	NLO	1.259	0.504
	NNLO	$0.997^{+0.053+0.002}_{-0.059-0.002}$	$0.399^{+0.021+0.001}_{-0.024-0.001}$
	NNLO + LL	$0.844^{+0.049+0.002}_{-0.054-0.002}$	$0.338^{+0.019+0.001}_{-0.022-0.001}$
$Z \to h_c + \gamma$	LO	19.231	7.707
	NLO	13.597	5.449
	NNLO	$10.261^{+0.557+0.021}_{-0.625-0.021}$	$4.112^{+0.223+0.008}_{-0.251-0.008}$
	NNLO + LL	$8.700^{+0.513+0.021}_{-0.575-0.021}$	$3.487^{+0.206+0.008}_{-0.230-0.008}$

TABLE V. Unpolarized (total) decay widths for $Z \to$ bottomonium $+ \gamma$ at various levels of accuracy. The source of the theoretical uncertainties is the same as that in Table IV.

Channel	Order	$\Gamma_{\text{total}}(\text{eV})$	$\text{Br}(\times 10^{-9})$
$Z \to \chi_{b0} + \gamma$	LO	0.598	0.240
	NLO	0.615	0.246
	NNLO	$0.704^{+0.012+0.001}_{+0.010-0.001}$	$0.282^{+0.005+0.001}_{-0.004-0.001}$
	NNLO + LL	$0.681^{+0.012+0.001}_{-0.010-0.001}$	$0.273^{+0.005+0.001}_{-0.004-0.001}$
$Z \to \chi_{b1} + \gamma$	LO	3.882	1.556
	NLO	3.771	1.511
	NNLO	$3.578^{+0.024+0.007}_{-0.028-0.007}$	$1.434^{+0.010+0.003}_{-0.011-0.003}$
	NNLO + LL	$3.676^{+0.025+0.007}_{-0.029-0.007}$	$1.473^{+0.010+0.003}_{-0.011-0.003}$
$Z \to \chi_{b2} + \gamma$	LO	1.323	0.530
	NLO	0.888	0.356
	NNLO	$0.762^{+0.032+0.001}_{-0.035-0.001}$	$0.305^{+0.013+0.001}_{-0.014-0.001}$
	NNLO + LL	$0.729^{+0.031+0.001}_{-0.035-0.001}$	$0.292^{+0.012+0.001}_{-0.014-0.001}$
$Z \to h_b + \gamma$	LO	3.964	1.589
	NLO	2.860	1.146
	NNLO	$2.419^{+0.093+0.005}_{-0.104-0.005}$	$0.969^{+0.037+0.002}_{-0.042-0.002}$
	NNLO + LL	$2.314^{+0.091+0.005}_{-0.102-0.005}$	$0.927^{+0.036+0.002}_{-0.041-0.002}$

several hundreds and thousands of charmonia and bottomonia production through $Z \to H + \gamma$. The signal for $Z \to \chi_{QJ} + \gamma$ production can be measured by probing χ_{QJ} with a recoiling hard photon, where χ_{QJ} can be reconstructed from their transition to $\gamma + J/\psi$ $(\gamma + \Upsilon)$ with $J/\psi(\Upsilon) \to \ell\ell$. Because of the low multiplicative branching ratio, and extra event-selection rules to suppress the backgrounds, it will be rather difficult to measure $Z \to \chi_{QJ} + \gamma$ in experiment. Alternatively, the χ_{QJ} may be reconstructed through its hadronic decays; however, the experimental measurements on $\chi_{QJ} + \gamma$ are still challenging. The condition for $Z \to h_Q + \gamma$ is even worse.

VI. SUMMARY

In summary, we study the exclusive decay processes of $Z \to \chi_{QJ}/h_Q + \gamma$ in the NRQCD framework. The amplitudes of all the helicity configurations and the unpolarized decay widths are evaluated up to $\mathcal{O}(\alpha_s^2)$. It is the first time that the NRQCD factorization for h_Q exclusive production at two-loop is verified explicitly. The LL of m_Z^2/m_Q^2 in the leading-twist SDCs are resummed to all orders of α_s by employing the LC factorization. We find the radiative corrections are considerable for χ_{Q2} and h_Q productions, while they are moderate or even minor for other channels. We also notice that the LL resummation can change the LO results by more than 25% for $\chi_{c0,2}$ and h_c production, and by around 50% for χ_{c1} production. However, effects of the LL resummation on the NLO and NNLO predictions are notably mitigated. We expect that several hundreds and thousands of charmonia and bottomonia will be produced through $Z \to H + \gamma$ at the proposed super-Z factories.

ACKNOWLEDGMENTS

The work of W.-L. S. and Y.-D. Z. is supported by the National Natural Science Foundation of China under Grants No. 11975187. The work of D. Y. is supported in part by the National Natural Science Foundation of China under Grants No. 11635009. We also wish to thank the computing platform of School of Physical Science and Technology of Southwest University for support.

APPENDIX: CONSTRUCTION OF HELICITY PROJECTORS

In this appendix, we present the helicity projectors $\mathcal{P}^{(H)}_{\lambda_1,\lambda_2}$, which have been used to compute the helicity amplitudes for $Z \to H(\lambda_1) + \gamma(\lambda_2)$ in Sec. III. We apply the similar technique applied in Refs. [49,50].

For the sake of convenience, we introduce an auxiliary transverse metric tensor and two auxiliary longitudinal vectors,

$$g_\perp^{\mu\nu} = g^{\mu\nu} + \frac{P^\mu P^\nu}{|\mathbf{P}|^2} - \frac{Q\cdot P}{m_Z^2|\mathbf{P}|^2}(P^\mu Q^\nu + Q^\mu P^\nu), \tag{A1a}$$

$$L_Z^\mu = \frac{1}{|\mathbf{P}|}\left(P^\mu - \frac{Q\cdot P}{m_Z^2}Q^\mu\right), \tag{A1b}$$

$$L_{\chi_{QJ}}^\mu = \frac{1}{|\mathbf{P}|}\left(\frac{P\cdot Q}{m_Z m_{\chi_{QJ}}}P^\mu - \frac{m_{\chi_{QJ}}}{m_Z}Q^\mu\right), \tag{A1c}$$

$$L_{h_Q}^\mu = \frac{1}{|\mathbf{P}|}\left(\frac{P\cdot Q}{m_Z m_{h_Q}}P^\mu - \frac{m_{h_Q}}{m_Z}Q^\mu\right), \tag{A1d}$$

where P and Q denote the momenta of the H meson and the Z boson, respectively. It is obvious that the transverse metric tensor satisfies

$$g_{\perp\mu\nu}P^\mu = g_{\perp\mu\nu}Q^\mu = 0, \tag{A2a}$$

$$g^\mu_{\perp\mu} = 2, \tag{A2b}$$

$$g_{\perp\mu\alpha}g^{\alpha\nu}_\perp = g_{\perp\mu\alpha}g^{\alpha\nu} = g^\nu_{\perp\mu}, \tag{A2c}$$

and the longitudinal vectors satisfy $L^\mu_Z Q_\mu = L^\mu_{\chi_{QJ}} P_\mu = L^\mu_{h_Q} P_\mu = 0$.

We enumerate all the eight helicity projectors

$$\mathcal{P}^{(\chi_{Q0})\mu\nu}_{0,1} = -\frac{1}{2}g^{\mu\nu}_\perp, \tag{A3a}$$

$$\mathcal{P}^{(\chi_{Q1})\mu\nu\alpha}_{1,1} = \frac{-1}{2m_Z|\mathbf{P}|}L^\mu_Z \epsilon^{\nu\alpha\rho\sigma}Q_\rho P_\sigma, \tag{A3b}$$

$$\mathcal{P}^{(\chi_{Q1})\mu\nu\alpha}_{0,1} = \frac{1}{2m_Z|\mathbf{P}|}L^\alpha_{\chi_{c1}} \epsilon^{\mu\nu\rho\sigma}Q_\rho P_\sigma, \tag{A3c}$$

$$\mathcal{P}^{(\chi_{Q2})\mu\nu\alpha\beta}_{2,1} = \frac{1}{4}(g^{\mu\nu}_\perp g^{\alpha\beta}_\perp - g^{\mu\alpha}_\perp g^{\nu\beta}_\perp - g^{\mu\beta}_\perp g^{\nu\alpha}_\perp), \tag{A3d}$$

$$\mathcal{P}^{(\chi_{Q2})\mu\nu\alpha\beta}_{1,1} = \frac{-1}{2\sqrt{2}}L^\mu_Z(g^{\nu\alpha}_\perp L^\beta_{\chi_{Q2}} + g^{\nu\beta}_\perp L^\alpha_{\chi_{Q2}}), \tag{A3e}$$

$$\mathcal{P}^{(\chi_{Q2})\mu\nu\alpha\beta}_{0,1} = \frac{-1}{2\sqrt{6}}g^{\mu\nu}_\perp(g^{\alpha\beta}_\perp + 2L^\alpha_{\chi_{Q2}}L^\beta_{\chi_{Q2}}), \tag{A3f}$$

$$\mathcal{P}^{(h_Q)\mu\nu\alpha}_{0,1} = -\frac{1}{2}g^{\mu\nu}_\perp L^\alpha_{h_Q}, \tag{A3g}$$

$$\mathcal{P}^{(h_Q)\mu\nu\alpha}_{1,1} = -\frac{1}{2}g^{\nu\alpha}_\perp L^\mu_Z. \tag{A3h}$$

If we express the decay amplitudes of $Z \to H(\lambda_1) + \gamma(\lambda_2)$ as

$$\mathcal{A}^{(\chi_{Q0})} = \mathcal{A}^{(\chi_{Q0})}_{\mu\nu}\epsilon^\mu_Z \epsilon^{*\nu}_\gamma, \tag{A4a}$$

$$\mathcal{A}^{(\chi_{Q1})} = \mathcal{A}^{(\chi_{Q1})}_{\mu\nu\alpha}\epsilon^\mu_Z \epsilon^{*\nu}_\gamma \epsilon^{*\alpha}_{\chi_{c1}}, \tag{A4b}$$

$$\mathcal{A}^{(\chi_{Q2})} = \mathcal{A}^{(\chi_{Q2})}_{\mu\nu\alpha\beta}\epsilon^\mu_Z \epsilon^{*\nu}_\gamma \epsilon^{*\alpha\beta}_{\chi_{Q2}}, \tag{A4c}$$

$$\mathcal{A}^{(h_Q)} = \mathcal{A}^{(h_Q)}_{\mu\nu\alpha}\epsilon^\mu_Z \epsilon^{*\nu}_\gamma \epsilon^{*\alpha}_{h_Q}, \tag{A4d}$$

where ϵ_Z and ϵ_γ represent the polarization vectors of the Z boson and the photon, respectively, the helicity amplitude can be computed through

$$\mathcal{A}^{(\chi_{Q0})}_{0,1} = \mathcal{P}^{(\chi_{Q0})\mu\nu}_{0,1}\mathcal{A}^{(\chi_{Q0})}_{\mu\nu}, \tag{A5a}$$

$$\mathcal{A}^{(\chi_{Q1})}_{0,1} = \mathcal{P}^{(\chi_{Q1})\mu\nu\alpha}_{0,1}\mathcal{A}^{(\chi_{Q1})}_{\mu\nu\alpha}, \tag{A5b}$$

$$\mathcal{A}^{(\chi_{Q1})}_{1,1} = \mathcal{P}^{(\chi_{Q1})\mu\nu\alpha}_{1,1}\mathcal{A}^{(\chi_{Q1})}_{\mu\nu\alpha}, \tag{A5c}$$

$$\mathcal{A}^{(\chi_{Q2})}_{2,1} = \mathcal{P}^{(\chi_{Q2})\mu\nu\alpha\beta}_{2,1}\mathcal{A}^{(\chi_{Q2})}_{\mu\nu\alpha\beta}, \tag{A5d}$$

$$\mathcal{A}^{(\chi_{Q2})}_{1,1} = \mathcal{P}^{(\chi_{Q2})\mu\nu\alpha\beta}_{1,1}\mathcal{A}^{(\chi_{Q2})}_{\mu\nu\alpha\beta}, \tag{A5e}$$

$$\mathcal{A}^{(\chi_{Q2})}_{0,1} = \mathcal{P}^{(\chi_{Q2})\mu\nu\alpha\beta}_{0,1}\mathcal{A}^{(\chi_{Q2})}_{\mu\nu\alpha\beta}, \tag{A5f}$$

$$\mathcal{A}^{(h_Q)}_{0,1} = \mathcal{P}^{(h_Q)\mu\nu\alpha}_{0,1}\mathcal{A}^{(h_Q)}_{\mu\nu\alpha}, \tag{A5g}$$

$$\mathcal{A}^{(h_Q)}_{1,1} = \mathcal{P}^{(h_Q)\mu\nu\alpha}_{1,1}\mathcal{A}^{(h_Q)}_{\mu\nu\alpha}. \tag{A5h}$$

[1] G. Aad *et al.* (ATLAS Collaboration), Phys. Rev. Lett. **114**, 121801 (2015).
[2] ATLAS Collaboration, CERN Report No. ATL-PHYS-PUB-2015-043, CERN, 2015.
[3] CMS Collaboration, CERN Report No. CMS-PAS-SMP-17-012, CERN, 2018.
[4] H. Baer, T. Barklow, K. Fujii, Y. Gao, A. Hoang, S. Kanemura, J. List, H. E. Logan, A. Nomerotski, M. Perelstein *et al.*, arXiv:1306.6352.
[5] A. Abada *et al.* (FCC Collaboration), Eur. Phys. J. C **79**, 474 (2019).
[6] J. B. Guimarães da Costa *et al.* (CEPC Study Group), arXiv:1811.10545.
[7] B. Guberina, J. H. Kuhn, R. D. Peccei, and R. Ruckl, Nucl. Phys. **B174**, 317 (1980).
[8] A. V. Luchinsky, arXiv:1706.04091.
[9] G. T. Bodwin, E. Braaten, and G. P. Lepage, Phys. Rev. D **51**, 1125 (1995); **55**, 5853(E) (1997).
[10] G. P. Lepage and S. J. Brodsky, Phys. Rev. D **22**, 2157 (1980).
[11] V. L. Chernyak and A. R. Zhitnitsky, Phys. Rep. **112**, 173 (1984).
[12] X. P. Wang and D. Yang, J. High Energy Phys. 06 (2014) 121.
[13] T. C. Huang and F. Petriello, Phys. Rev. D **92**, 014007 (2015).

[14] Y. Grossman, M. König, and M. Neubert, J. High Energy Phys. 04 (2015) 101.
[15] G. T. Bodwin, H. S. Chung, J. H. Ee, and J. Lee, Phys. Rev. D **97**, 016009 (2018).
[16] H. Dong, P. Sun, B. Yan, and C. P. Yuan, Phys. Lett. B **829**, 137076 (2022).
[17] G. Chen, X. G. Wu, Z. Sun, S. Q. Wang, and J. M. Shen, Phys. Rev. D **88**, 074021 (2013).
[18] G. Chen, X. G. Wu, Z. Sun, X. C. Zheng, and J. M. Shen, Phys. Rev. D **89**, 014006 (2014).
[19] Z. Sun, X. G. Wu, G. Chen, Y. Ma, H. H. Ma, and H. Y. Bi, Phys. Rev. D **89**, 074035 (2014).
[20] Y. Jia and D. Yang, Nucl. Phys. **B814**, 217 (2009).
[21] A. V. Efremov and A. V. Radyushkin, Phys. Lett. **94B**, 245 (1980).
[22] H. E. Haber, arXiv:hep-ph/9405376.
[23] M. Jacob and G. C. Wick, Ann. Phys. (N.Y.) **7**, 404 (1959).
[24] V. L. Chernyak and A. R. Zhitnitsky, Sov. J. Nucl. Phys. **31**, 544 (1980).
[25] S. J. Brodsky and G. P. Lepage, Phys. Rev. D **24**, 2848 (1981).
[26] W. L. Sang, F. Feng, and Y. Jia, J. High Energy Phys. 10 (2020) 098.
[27] A. H. Hoang and P. Ruiz-Femenia, Phys. Rev. D **74**, 114016 (2006).
[28] T. Hahn, Comput. Phys. Commun. **140**, 418 (2001).
[29] V. Shtabovenko, R. Mertig, and F. Orellana, Comput. Phys. Commun. **207**, 432 (2016).
[30] F. Feng and R. Mertig, arXiv:1212.3522.
[31] J. G. Korner, D. Kreimer, and K. Schilcher, Z. Phys. C **54**, 503 (1992).
[32] M. Beneke and V. A. Smirnov, Nucl. Phys. **B522**, 321 (1998).
[33] F. Feng, Comput. Phys. Commun. **183**, 2158 (2012).
[34] A. V. Smirnov, Comput. Phys. Commun. **189**, 182 (2015).
[35] H. H. Patel, Comput. Phys. Commun. **197**, 276 (2015).
[36] X. Liu, Y. Q. Ma, and C. Y. Wang, Phys. Lett. B **779**, 353 (2018).
[37] X. Liu, Y. Q. Ma, W. Tao, and P. Zhang, Chin. Phys. C **45**, 013115 (2021).
[38] X. Liu and Y. Q. Ma, Phys. Rev. D **105**, L051503 (2022).
[39] X. Liu and Y. Q. Ma, Comput. Phys. Commun. **283**, 108565 (2023).
[40] M. Fael, K. Schönwald, and M. Steinhauser, J. High Energy Phys. 10 (2020) 087.
[41] W. L. Sang and Y. Q. Chen, Phys. Rev. D **81**, 034028 (2010).
[42] P. A. Zyla *et al.* (Particle Data Group), Prog. Theor. Exp. Phys. **2020**, 083C01 (2020).
[43] K. G. Chetyrkin, J. H. Kuhn, and M. Steinhauser, Comput. Phys. Commun. **133**, 43 (2000).
[44] G. P. Lepage and S. J. Brodsky, Phys. Lett. **87B**, 359 (1979).
[45] G. T. Bodwin, H. S. Chung, J. H. Ee, and J. Lee, Phys. Rev. D **95**, 054018 (2017).
[46] Q. F. Sun, F. Feng, Y. Jia, and W. L. Sang, Phys. Rev. D **96**, 051301 (2017).
[47] E. J. Eichten and C. Quigg, Phys. Rev. D **52**, 1726 (1995).
[48] H. S. Chung, J. High Energy Phys. 09 (2021) 195.
[49] J. Xu, H. R. Dong, F. Feng, Y. J. Gao, and Y. Jia, Phys. Rev. D **87**, 094004 (2013).
[50] Y. D. Zhang, F. Feng, W. L. Sang, and H. F. Zhang, J. High Energy Phys. 12 (2021) 189.